Journal of Photochemistry and Photobiology A: Chemistry 216 (2010) 261–267

Contents lists available at ScienceDirect

Journal of Photochemistry and Photobiology A: Chemistry

journal homepage: www.elsevier.com/locate/jphotochem

Adsorption and photocatalytic bleaching of acid orange 7 on P25 titania

Christopher O'Rourke, Andrew Mills*

Department of Pure and Applied Chemistry, University of Strathclyde, Glasgow G11XL, UK

ARTICLE INFO

Article history:
Available online 14 July 2010

Keywords:
Photocatalysis
CD-MUSIC
Adsorption
Photobleaching
Acid orange 7

ABSTRACT

The observed adsorption of acid orange 7, $AO7^-$, on P25 titania over a range of pH values (pH 2–8) gives a good fit to data generated using a charge distribution, multisite complexation, i.e. CD-MUSIC, model, modified for aggregated dye adsorption. For this system the model predicts that both the apparent dark Langmuir adsorption constant, K_L, and the number of adsorption sites, n_o, increase with decreasing pH, and are negligible above pH 6. At pH 2 the CD-MUSIC model predicts the fraction of singly co-ordinated sites occupied by the dye, f_{AO7}, is *ca.* 32% under the *in situ* monitoring experimental conditions used in this work to study the photocatalytic bleaching of $AO7^-$ under UV light illumination ($[TiO_2] = 20\,mg\,dm^{-3}$; $[AO7^-]_{total} = 4.86 \times 10^{-5}$ M). Although $AO7^-$ adsorption on P25 titania is insignificant above pH 6 and increases almost linearly and markedly below this pH, the measured initial rate of bleaching of $AO7^-$, photocatalysed by titania using UV appears to only *increase* modestly (<factor of 2) over the pH range 2–10 studied. Possible reasons for the lack of a strong dependency of initial rate of photobleaching, r_i, upon f_{AO7} are discussed briefly. In contrast, the rate of bleaching of $AO7^-$ via a visible light driven, dye-sensitised process, shows some correlation with the CD-MUSIC model-calculated variation of f_{AO7} as a function of pH. Such a correlation follows from the basic assumption that only dye molecules that are in direct contact with the surface can undergo photodegradation via a dye-sensitised route.

1. Introduction

Semiconductor photocatalysis (SPC) is an expanding field based on an apparently simple set of processes [1]. Thus, ultra-band-gap irradiation of the semiconductor generates an electron–hole pair which may recombine in the bulk or migrate to the surface. At the surface they may recombine or undergo reactions with an electron acceptor, such as O_2, and an electron donor, such as an organic. In the latter case, the semiconductor will have acted as a photocatalyst for the oxidation of the organic by O_2 and extensive research has shown that titania (TiO_2) is particularly effective in this role [2]. Indeed, the list of organics that can be mineralised via SPC is extensive and includes many common water pollutants, such as: pesticides, surfactants and dyes [3]. In the case of dyes, one of the most popular ones used in SPC is the anionic azo dye, $AO7^-$, which is believed to adsorb as a bidentate ligand onto the surface of TiO_2 [4–6].

With the increasing research into semiconductor photocatalysis, many new materials and commercial products have emerged. A popular method used to assess rapidly and simply the photocatalytic activity of such new photocatalytic materials is to monitor its ability to promote the photobleaching of a dyestuff, such as $AO7^-$ [2,7,8], via SPC. However, such test systems are not as simple as at first they might seem. For example, in the case of $AO7^-$, although the dye is usually (for solutions in which $10 > pH > 2$) in its anionic form, the sign and size of the charge on the surface of the semiconductor photocatalyst under test is usually pH, type of electrolyte, and ionic strength dependent. As a consequence, the amount of dye adsorbed onto the surface, due to electrostatic attractive forces, is also pH and ionic strength dependent. For example, the adsorption of $AO7^-$ on the photocatalyst under test will be significant if the pH of the test solution is much lower than the point of zero charge (*PZC*) of the photocatalyst and negligible if the $pH \gg PZC$ [7]. Indeed, in a recent paper, Bourikas et al. modelled the adsorption features of $AO7^-$ on the surface of that most notable of semiconductor photocatalysts, Degussa P25, using a charge distribution, multisite complexation (CD-MUSIC) model, which takes into account the different types of surface species on the metal oxide [6]. Amongst other things this model showed, as noted by others, that decreasing the solution pH with respect to the *PZC* of the titania photocatalyst (pH 6.6), increases the apparent dark Langmuir adsorption constant, K_L, and the apparent number of adsorption sites, n_o, exhibited by $AO7^-$ adsorption isotherms [6,9].

As a consequence of the above it is clear that the initial pH of the reaction solution is important when using such a test system. This feature is further complicated by the fact that the photobleaching process often generates acidic species (and ultimately mineral acids) which will reduce the pH of the reaction solution as the photoreaction proceeds [10]. This effect is of particular significance if the initial pH is near neutral, or 'natural pH', as is often the case in

* Corresponding author. Tel.: +44 0 141 548 2458; fax: +44 0 548 4822.
E-mail address: a.mills@strath.ac.uk (A. Mills).

1010-6030/$ – see front matter © 2010 Elsevier B.V. All rights reserved.
doi:10.1016/j.jphotochem.2010.07.006

SPC activity measurement studies [11,12]. In the case of AO7$^-$ the complete photomineralisation process, by SPC, is summarised by the following reaction equation:

$$C_{16}H_{11}N_2NaO_4S + 21O_2 \xrightarrow[h\nu \geq E_{bg}]{\text{semiconductor}} 16CO_2 + 2HNO_3 + NaHSO_4 + 4H_2O \quad (1)$$

It should also be recognised, when using a dye test system for assessing SPC activity, that dye photobleaching can also occur via a dye photosensitised process in which the electronically excited state of the dye injects an electron into the conduction band of the semiconductor to produce an oxidised dye radical which is unstable and capable of decomposing to bleached products [11,13–15]. The injected electron can also promote this process via its subsequent reaction with O_2 to produce a number of different oxidising species, such as hydrogen peroxide. In order to discriminate between these two very different processes, and so be able to comment on SPC activity, careful selection of the wavelength(s) of excitation must be made. The importance of achieving this discrimination is most pertinent when visible light photocatalytic activity is assessed, as noted by Ohtani and his co-workers [14]. Fortunately, AO7$^-$ has a minimum in its UV absorption spectrum around the wavelength of UV light usually used (365 nm from a BL or BLB lamp) for assessing the activity of UV-absorbing semiconductor photocatalysts such as P25 TiO_2. The quantum efficiency of the dye-sensitised reaction is also much lower than that for photocatalytic reaction (1) using P25. For example, in contrast to work with BLBs, when using the same wattage visible fluorescent tubes as BLBs, but filtered to remove the UV, there is little evidence of bleaching via dye sensitisation when studying the AO7$^-$/P25 titania system.

Finally, a less well recognised, complicating, feature involving the use of dyes to assess photocatalytic activity is the tendency of many dyes (including the most popular test dyes) to aggregate even at low concentrations (<10^{-4} M) to form multimers such as dimers, trimers, etc. AO7$^-$ is particularly interesting in this regard since its aggregated forms have very similar UV/Vis characteristics to its monomeric form and higher aggregates than dimer or trimer [16–20], including colloidal AO7$^-$ give only 'a small spectral perturbation' [20]! As a consequence, it is not surprising that the formation of these aggregates is not commonly recognised in SPC activity measurements using this dye.

In this paper we investigate the effect of AO7$^-$ aggregation on the CD-MUSIC model of its adsorption on P25 TiO_2 and examine how the results relate to the SPC activity of P25 as a function of pH.

2. Experimental

All chemicals were purchased from Aldrich Chemicals and used as received, unless stated otherwise. The P25 TiO_2 used was a gift from the Degussa-Evonik Corporation. The water used to make up solutions was double distilled and deionised.

All UV irradiations were conducted using two 8W black light blue (BLB) fluorescent tubes with an output maximum at 365 nm and a typical UV irradiance of 2 mW cm^{-2}. All visible irradiations were carried out using a 180 W Xe arc lamp fitted with a 400 nm cut-off filter to remove the UV component of the light. In a typical irradiation, 1.7 mg of the sodium salt of AO7$^-$ were dissolved in 100 cm^3 of a 0.01 M NaCl solution and its pH adjusted to the desired value using small amounts of 0.1 M solutions of NaOH or HCl. To this solution were added 2 mg of P25 and the dispersion was then subjected to ultrasound from a bath for 10 min to ensure complete dispersion. For each dispersion, 3.5 cm^3 of the dispersion were added to a quartz 1 cm cuvette and left stirring for 1 h before being irradiated. The photobleaching of the dye was monitored as a function of irradiation time via UV/Vis spectrophotometry and the absorbance at the wavelength of maximum absorbance, 484 nm. The above low concentrations of AO7$^-$ (4.86×10^{-5} M) and, particularly, TiO_2, (20 mg dm^{-3}) allow for the *in situ* monitoring of the photobleaching of AO7$^-$, i.e. no filtering of solution is required. It is, however, also quite common [12,15] to use much high concentrations (e.g. $[AO7^-]_{total} = 8.57 \times 10^{-4}$ M; $[TiO_2] = 750$ mg dm^{-3}), which, as a consequence, require filtering before being assessed spectrophotometrically; and we shall refer to this method as *ex situ* monitoring. Over the pH range studied (pH 2–10) there is no significant change in the UV/Vis absorption spectrum of the AO7$^-$ solution (4.86×10^{-5} M).

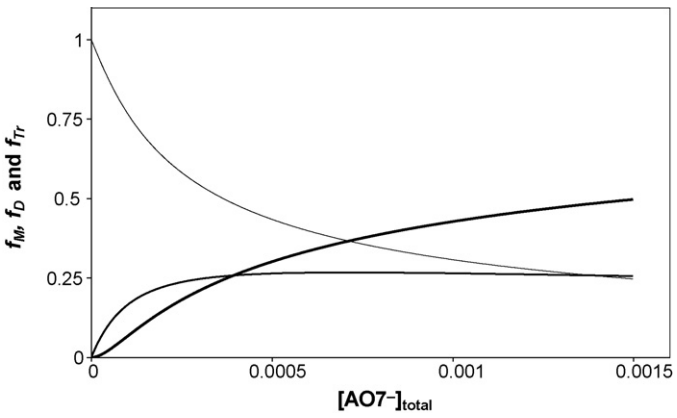

Fig. 1. Fractions of AO7$^-$, in the form of a monomer (thin solid line), dimer (broken line) and trimer (thick solid line), in solution as a function the total dye concentration, $[AO7^-]_{total}$, calculated using the dimerisation and trimerisation constants reported Ghosh and Mukerjee [19].

MUSIC [21] and CD-MUSIC [6,22] calculations were performed using appropriate in-house generated macros run in Excel™. Details of the key reaction equilibria and mass balance equations, the model constants and optimised parameter values are given in the text, with further details in Appendix A.

3. Aggregation of AO7$^-$

The aggregation of azo dyes, such as AO7$^-$, has been well studied [16–20], including by Ghosh and Mukerjee [19], who studied the dimerisation and trimerisation of many dyes, including AO7$^-$ via UV/Vis spectrophotometry, and the following equilibria:

$$2AO7^- \overset{K_D}{\longleftrightarrow} (AO7^-)_2 \quad (2)$$

$$(AO7^-)_2 + AO7^- \overset{K_{Tr}}{\longleftrightarrow} (AO7^-)_3 \quad (3)$$

These workers report values of 1400 M^{-1} and 3500 M^{-1} for the equilibria constants, K_D and K_{Tr} and others [16–18] have reported similar values (*e.g.* 953, 1030, 1320 M^{-1}) for K_D. Using the values of K_D and K_{Tr} reported by Ghosh and Mukerjee [19] the fractions of AO7$^-$ in its monomeric, dimeric and trimeric form, i.e. f_M, f_D and f_{Tr}, present in different total dye concentrations, $[AO7^-]_{total}$, spanning the range 0–1.5 mM, were calculated and the results of this work are illustrated in Fig. 1. Thus, at a typical $[AO7^-]_{total}$ used for *in situ* SPC studies, where the absorbance of the solution has a value of ca. 1 in a 1 cm cell, i.e. 4.86×10^{-5} M, the values of f_M, f_D and f_{Tr} are ca. 0.78, 0.1 and 0.02, respectively. From these values it is clear the level of dimer in solution is not insignificant even at this low $[AO7^-]_{total}$. It should also be noted, that the fractions of these aggregated species increases with increasing $[AO7^-]_{total}$, so that at an $[AO7^-]_{total} = 8.57 \times 10^{-4}$ M – not atypical of the dye concentrations used in *ex situ* monitored SPC studies – the values of these fractions are increased to:0.33, 0.27 and 0.40, respectively, which are disturbingly appreciable levels!

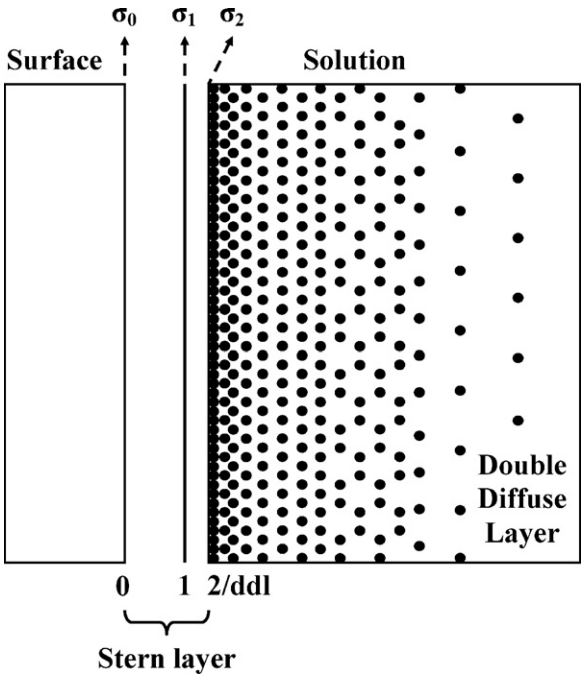

Fig. 2. Schematic diagram illustrating the basic features of a three plane model of a metal oxide–electrolyte interface with inner sphere complex formation at the 1-plane and outersphere complex formation with the counterions at the head of the *ddl* in the 2-plane.

4. MUSIC and CD-MUSIC models

The most commonly used model of the charging behaviour of metal oxides has been the one site/two-pK_a model [23] which assumes a single surface site type which can absorb or desorb a proton, i.e. for TiO_2

$$TiO^- + 2H^+ \overset{K_{a1}}{\longleftrightarrow} TiOH + H^+ \overset{K_{a2}}{\longleftrightarrow} TiOH_2^+ \quad (4)$$

where K_{a1} and K_{a2} are the sequential acid association constants for the TiO^- surface species. This simple model reflects the amphoteric nature of the metal oxide, but not the different types of surface site which are known from surface spectroscopy studies [21–23].

A more recent, and increasing popular, model that takes such species into account is called the multisite complexation (MUSIC) model [2,23]. In the case of titania, the MUSIC model identifies singly ($TiOH^{-1/3}$) and doubly ($Ti_2O^{-2/3}$) co-ordinated surface groups as responsible for the observed charging behaviour of the titania surface via the following protonation reactions:

$$TiOH^{-1/3} + H^+ \overset{K_{H1}}{\longleftrightarrow} TiOH_2^{+2/3} \quad (5)$$

$$Ti_2O^{-2/3} + H^+ \overset{K_{H2}}{\longleftrightarrow} Ti_2OH^{+1/3} \quad (6)$$

where K_{H1} and K_{H2} are the acid association constants for these two surface species. Other work indicates that these two constants have similar values and so, for simplicity, are usually assumed equal and represented by one parameter, K_H [21,23]. It is also usual to assume that the densities of the singly and doubly co-ordinated sites, $TiOH^{-1/3}$ and $Ti_2O^{-2/3}$, are the same and equal to N_S [21,23].

Hydrated counterions of the background electrolyte have a minimum distance of approach to the surface and so form a diffuse double layer (*ddl*) with its head at the 2-plane illustrated in Fig. 2. The hydrated ions at the 2-plane are usually treated as point charges, which form outersphere, ion-pair complexes with the surface groups. The ion-pair reactions of the surface groups with these

Table 1
Parameters used in the MUSIC and Monomer and Multimer dye CD-MUSIC Models (at 298 K).

Parameter	Value	Parameter	Value
MUSIC (Basic Stern) model			
C ($F\,m^{-2}$)	0.9	$\log K_H$	6.6
$\log K_{Na}$	−0.5	$\log K_{Cl}$	−1.1
N_S (nm^{-2})	5.6		
Monomer and Multimer Dye CD-MUSIC models			
C_1 ($F\,m^{-2}$)	1.1	$\log K_{AO7\text{-}in}$ (ref [6])	15.1
C_2 ($F\,m^{-2}$)	5.0	$\log K_{AO7\text{-}in}$ (this work)	14.54
General data			
A (m^2/g)	50	K_D (M^{-1})	1400
K_{Tr} (M^{-1})	3500		

hydrated ions at the head of the *ddl* are as follows:

$$TiOH^{-1/3} + C^+ \overset{K_{C1}}{\longleftrightarrow} TiO^{-1/3} - C^+ \quad (7)$$

$$TiOH_2^{+2/3} + A^- \overset{K_{A1}}{\longleftrightarrow} TiOH_2^{+2/3} - A^- \quad (8)$$

$$Ti_2O^{-2/3} + C^+ \overset{K_{C2}}{\longleftrightarrow} Ti_2O^{-2/3} - C^+ \quad (9)$$

$$Ti_2OH^{+1/3} + A^- \overset{K_{A2}}{\longleftrightarrow} Ti_2OH^{+1/3} - A^- \quad (10)$$

where C^+ and A^- are the hydrated cations and anions of the counterions at the head of the *ddl* and K_{C1}, K_{C2}, K_{A1} and K_{A2} are the relevant ion-pair complexation constants. As with K_{H1} and K_{H2}, it is usual to assume that $K_{C1} = K_{C2} = K_C$ and $K_{A1} = K_{A2} = K_A$ [21,23].

The above, simple basic Stern MUSIC model has been used by Bourikas et al. to model very effectively the observed primary charging behaviour of titania, including P25, as a function of pH, for a wide variety of different electrolytes [21]. In this work, the surface charge (σ_o) versus pH plots for P25 TiO_2 in solutions of different [NaCl] were generated using the MUSIC model and the parameters in Table 1. The results are illustrated in Fig. 3 and show that with increasing difference between the solution pH and the *PZC* of P25 TiO_2 (i.e. $\Delta pH = pH - PZC$) the surface charge either becomes increasingly positive (for increasing negative values of ΔpH) or negative (for increasing positive ΔpH). This model assumes that the tendency of the particles to aggregate – which is greatest at the *PZC* – does not reduce the effective number of adsorption sites available and this is supported by the work of many workers [22,23] in their excellent fits of the Stern model generated curves to the observed charging behaviour of many oxides, including TiO_2, in well-stirred systems. Although particle size measurements were not performed as part of this work, the absorption spectra of the titania dispersions with and without dye were recorded, since the turbidity of these dispersions, as measured by the absorbance at 800 nm say, provides

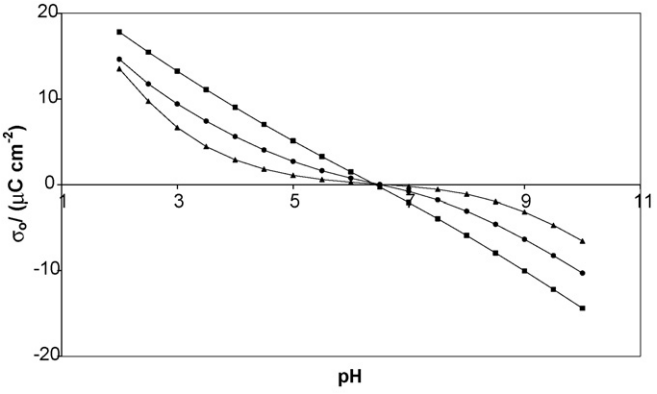

Fig. 3. Charging behaviour of P25 titania at various [NaCl] levels as a function of pH, as calculated using the MUSIC model and the parameters listed in Table 1. The [NaCl] values used were: 0.1 (■), 0.01 (●) and 0.001 (▲) M, respectively.

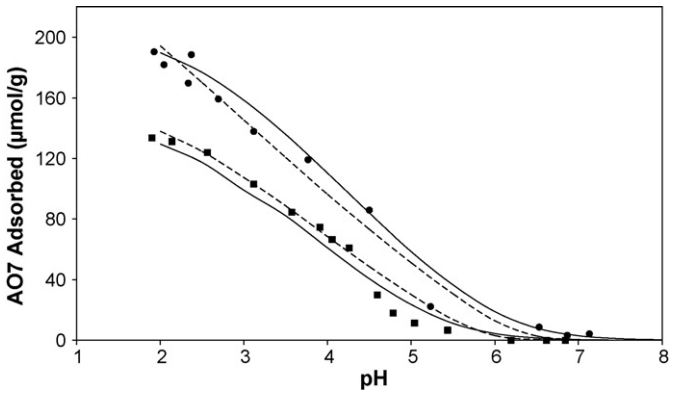

Fig. 4. Adsorption edge data for $AO7^-$ on P25 titania measured under *ex situ* conditions ($[TiO_2] = 750\ mg\ dm^{-3}$) reported by Bourikas et al. [6], for $[AO7^-]_{total}$ values of: 8.56×10^{-4} M (●) and 1.43×10^{-4} M (■). The solid lines were those calculated using the CD-MUSIC model (assuming all free and adsorbed dye is monomeric) and the constants given in Table 1; the curves are identical to those reported earlier by Bourikas et al. [6]. The broken lines were those calculated using the revised multimer CD-MUSIC model and the constants given in Table 1.

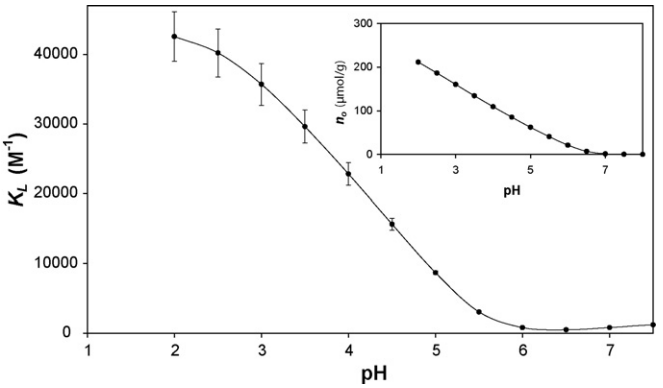

Fig. 5. Plots of the apparent values of the Langmuir adsorption constant, K_L, (main diagram) and the total number of surface sites available for innersphere complex formation, n_o, (insert diagram) as a function of pH. Each K_L and n_o data set was obtained using the multimer CD-MUSIC model to predict the adsorption isotherm at a pH, which was then analyse as if they were Langmuir-type isotherms, so as to reveal values for K_L and n_o.

a reasonable guide to the degree of dispersion of the particles. In our work it was found the absorbance of the P25 dispersion at 800 nm, with and without the dye (17 mg L^{-1}) did not vary over the pH range 2–10, thereby indicating a reasonably consistent dispersion of the titania, with and without dye, at all pHs studied.

It follows from the above that, if the adsorption of $AO7^-$ is due mainly to electrostatic attractive forces then the values of K_L, and n_o for $AO7^-$ adsorption would be expected to increase with increasing negative ΔpH and become increasingly negligible for increasing positive values of ΔpH. This simple model provides a rationale for the well established observation that 'cationic dyes bind [on metal oxide semiconductor photocatalysts] at pH values greater than the *PZC*, while anionic dyes show the opposite trend' [7].

The above simple MUSIC model has been extended to include surface (innersphere) complexes which form between the surface species and a strongly binding species, such as a dye [6]. Unlike weak, outersphere complexes, part of the charge of the innersphere complexes is attributed to the surface (the 0-plane in Fig. 2) and the remaining part resides in the first plane (the 1-plane) at a distance from the surface but before the *ddl*. The capacitance of the basic Stern layer, *C*, divides into two when innersphere complexes are formed, with the inner- and outer-layer capacitances, C_1 and C_2, related to *C* via:

$$\frac{1}{C} = \frac{1}{C_1} + \frac{1}{C_2} \tag{11}$$

The charge densities and potentials of the three (0-, 1- and 2-) planes are: σ_o, σ_1 and σ_2 and ψ_1, ψ_2 and ψ_d, respectively (see Fig. 2).

It is generally assumed that only the singly co-ordinated surface groups form innersphere complexes with anions [6]. Thus, assuming $AO7^-$ forms a bidentate innersphere complex with $TiOH^{-1/3}$, as suggested by the work of others [16–20], the key reaction involving $AO7^-$ adsorption at such sites is:

$$2TiOH^{-1/3} + 2H^+ + AO7^- \overset{K_{AO7}}{\longleftrightarrow} Ti_2AO7^{+1/3} + 2H_2O \tag{12}$$

The CD-MUSIC approach, coupled with reactions (4)–(12) and the key model parameters in Table 1, were used by Bourikas et al. (with $\log K_{AO7\text{-in}} = 15.1$, *vide infra*) to generate the solid line fits to their adsorption edge data recorded for $AO7^-$ on P25 that are illustrated in Fig. 4. Further details of how the CD-MUSIC model was used to generate these curves are given in Appendix A. The above fit to the data is good, but is based on the erroneous, but commonly made, assumption that the dye is monomeric at all the concentrations used to generate the data in Fig. 4. An obvious and simple improvement to this model is to assume that the $TiOH^{-1/3}$ surface species adsorb the monomer, dimer and trimer forms of $AO7^-$ equally well (not including the electrostatic element), i.e. for the relevant adsorption processes:

$$2TiOH^{-1/3} + 2H^+ + (AO7^-)_2 \overset{K'_{AO7}}{\longleftrightarrow} Ti_2(AO7)_2^{-2/3} + 2H_2O \tag{13}$$

$$2TiOH^{-1/3} + 2H^+ + (AO7^-)_3 \overset{K''_{AO7}}{\longleftrightarrow} Ti_2(AO7)_3^{-5/3} + 2H_2O \tag{14}$$

$K'_{AO7} = K''_{AO7} = K_{AO7}$. Note that K_{AO7} is an apparent constant in which the concentrations of surface sites are in units of M. In contrast, in Table 1, intrinsic constants are reported, i.e. ones in which the surface sites are expressed as mole fractions, which renders them independent of experimental conditions such as ρ, the solid solution ratio (in this case $[TiO_2]$ in g dm^{-3}) and *A*, the specific surface area ($m^2\ g^{-1}$). As a consequence, because it is for a bidentate reaction, K_{AO7} is related to the intrinsic constant, $K_{AO7\text{-in}}$ (in Table 1) via the following expression:

$$K_{AO7} = \frac{K_{AO7\text{-in}}}{(\rho A N_S)} \tag{15}$$

The solid lines illustrated in Fig. 4, showing an improved fit, were generated using: the above revised (multimer) version of the CD-MUSIC model employed by Bourikas et al. [6], the constants given in Table 1, with a revised value for K_{AO7} ($\log K_{AO7\text{-in}} = 14.54$), and the values of K_D and K_{Tr} reported by Ghosh and Mukerjee [19] and given earlier. These lines reveal an encouragingly overall improved fit to the adsorption edge data.

The above multimer CD-MUSIC model can also be used to generate adsorption isotherms for $AO7^-$ as a function of pH which can be subsequently analysed as if they were Langmuir adsorption curves, so as to generate apparent values of K_L, and n_o as a function of pH, plots of which are illustrated in Fig. 5. These plots reveal the not too surprising finding that K_L, and n_o increase with increasing negative ΔpH and are negligible for positive values of ΔpH; trends that have been observed by others [12,24].

5. $AO7^-$ as a test dye for assessing photocatalyst activity with UV light

In a series of experiments carried out under *in situ* monitoring conditions ($[TiO_2] = 20\ mg\ dm^{-3}$; $[AO7^-]_{total} = 4.86 \times 10^{-5}$ M) the initial rates of $AO7^-$ bleaching, r_i, photosensitised by UV-excited titania, were measured as a function of pH and the results

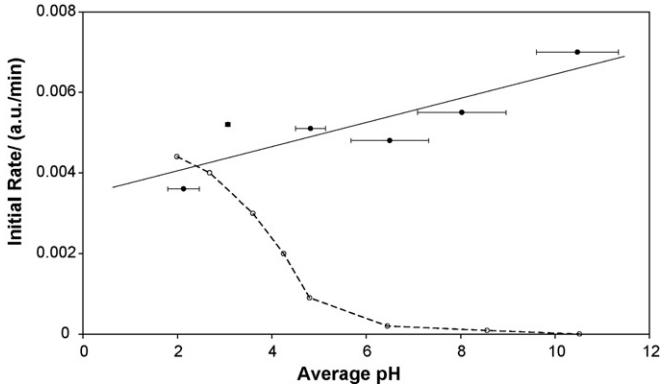

Fig. 6. Measured initial rate of photobleaching of $AO7^-$ (in units of absorbance units at 484 nm per min, i.e. au min^{-1}) as a function of pH for experiments conducted under *in situ* conditions ($[TiO_2] = 20\ mg\ dm^{-3}$; $[AO7^-]_{total} = 4.86 \times 10^{-5}$ M), with [NaCl] = 0.01 M, using either: (●) two 8 W BLB lamps (UVA: 2 mW cm^{-2}) or (○) a 180 W Xe arc lamp with a 400 nm filter (i.e. a visible – no UV – light source).

of this work are illustrated in Fig. 6. Surprisingly, these results reveal the rate increases by less than a factor of 2 over the pH range 2 to 10 and are not too dissimilar to those reported by others using P25 TiO_2 as the semiconductor photocatalyst [15,25]. For example, using an *ex situ* method ($[TiO_2] = 750\ mg\ dm^{-3}$; $[AO7^-]_{total} = 8.57 \times 10^{-4}$ M), Verykios et al. found the rate of photobleaching under solar-simulator Xe-arc light irradiation to be pH independent over the range pH 2–9, but faster at pH 10–12 [15]. Palmisano and his co-workers reported, also using an *ex situ* method ($[TiO_2] = 200\ mg\ dm^{-3}$; $[AO7^-]_{total} = 2.86 \times 10^{-5}$ M), that whilst the rate of photobleaching of $AO7^-$ under solar light irradiation dipped at pH 6, at pH 2 and 11 the rates were similar [25]. Note that the results from the above two reports are complicated by the fact that dye bleaching can occur by both semiconductor photocatalysis and dye photosensitisation as solar, or solar simulated, light was used.

The multimer CD-MUSIC model reported here can be used to estimate the total fraction of singly co-ordinated sites occupied by the dye, f_{AO7}, as a function of solution pH, under the *ex situ* measurements employed in this work, and the results are illustrated in Fig. 7. This plot shows that, as expected, f_{AO7} increases markedly with increasingly negative ΔpH; note also that the model predicts this effect is even more pronounced under *ex situ* monitoring conditions, since f_{AO7} increases significantly with increasing $[AO7^-]_{total}$. The results illustrated in Fig. 7 do not provide a ready explanation of the kinetic results illustrated in Fig. 6 for UV irradiation of the $AO7^-/TiO_2$ system, since it would seem reasonable to expect r_i to be related to f_{AO7}. The reasons as to why that this is not the case are unclear. The simplest explanation is that the photocatalysed bleaching of $AO7^-$ occurs via the doubly co-ordinated sites, i.e. $Ti_2O^{-2/3}$, since – according to the CD_MUSIC model – dye adsorption (via innersphere complex formation) does not occur at these sites at any pH. However, a number of alternative explanations are also possible. Interestingly, a modest variation in r_i (initial photocatalytic rate) as a function of pH appears a common feature of both anionic and cationic (such as methylene blue) dyes when used to assess the activity of P25 titania [12]. Clearly, further work is required to ascertain the underlying cause(s) for this notable, apparently common, largely indifferent variation in rate as a function of pH for anionic and cationic dyes when used to test titania under UVSPC conditions.

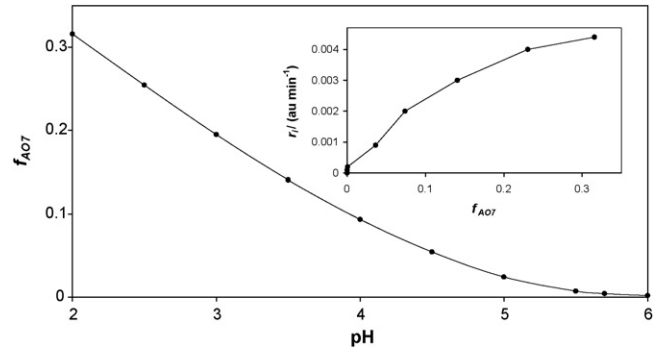

Fig. 7. Multimer CD-MUSIC model-calculated values of the fraction of singly co-ordinated surface sites on P25 titania with adsorbed $AO7^-$, f_{AO7}, as a function of pH. The insert plot is of the r_i values from Fig. 6, for visible light versus the value of f_{AO7} at the associated pH.

6. $AO7^-$ sensitised bleaching using visible light

As noted earlier, $AO7^-$ can also be photobleached via a dye-sensitised process in which the electronically excited state of the dye, $AO7^{-*}$, injects an electron into the conduction band of the titania to produce an oxidised dye radical, $AO7^{\bullet}$, which is unstable and capable of decomposition into colourless products, i.e.

$$AO7^{-}* + TiO_2 \rightarrow AO7^{\bullet} + TiO_2(e^-) \quad (16)$$

Since $AO7^-$ does not absorb strongly in the UV, this dye-sensitised process is most easily and usually demonstrated using an intense visible light, such as provided by a Xe-arc light. Thus, using the same *in situ* reaction conditions as described previously, but with a 180 W Xe arc light, combined with a 400 nm cut-off filter, the initial rate of dye photobleaching was measured as a function of pH and the results are also illustrated in Fig. 6. These results show the rate increases from a small value at pH 6 to a significant rate at pH 2, much like the fraction of sites occupied by adsorbed dye on the TiO_2 increases with decreasing pH (see Fig. 7). Indeed, the insert diagram in Fig. 7, which shows a plot of r_i values measured using visible light at different pHs versus the multimer CD-MUSIC model-calculated value of f_{AO7}, reveals a clear, if not simple, correlation between the two parameters. This correlation seems appropriate given the nature of the key process, i.e. reaction (16), and its implication that only dye molecules that are in direct contact with the surface can undergo photodegradation via such a dye-sensitised route [26]. Note however, at surface coverages approaching or exceeding a monolayer, as might be expected using high dye concentrations, dye excited state annihilation and self-quenching processes can compete with the charge injection process and so decrease the efficiency of dye-sensitised photobleaching [26]. The latter effect may be responsible for the apparent negative deviation from linearity in the insert plot at high values of r_i versus f_{AO7}.

7. Conclusions

The observed adsorption of $AO7^-$ on P25 titania over a range of pH values (pH 2–8) is well described using a CD-MUSIC model which accounts for dye aggregation in solution and subsequent adsorption of these aggregates. The model predicts the apparent dark Langmuir adsorption constant, K_L, and the number of adsorption sites, n_o, increases with decreasing pH, as has been observed by others [12,24]. The rate of bleaching of $AO7^-$, photocatalysed by titania using UV light, appears to *increase* modestly (by a factor < 2) over the pH range 2–10, despite the fact that $AO7^-$ adsorption on P25 titania is not significant above pH 6 and increases almost linearly and markedly below pH 6, covering ca. 32% of the singly co-ordinated surface sites at pH 2 under *in situ* experimental conditions ($[TiO_2] = 20\ mg\ dm^{-3}$; $[AO7^-]_{total} = 4.86 \times 10^{-5}$ M). The reasons for the lack of a strong dependency of initial rate of photobleaching upon f_{AO7} remain unclear. In contrast, the initial rate

Table A1
Surface speciation for the adsorption of $AO7^-$ on the surface of P25 titania.

	Dissolved component				Surface component		Electrostatic component			
Surface species	H^+	Na^+	Cl^-	$AO7^-$	$TiOH^{-1/3}$	$Ti_2O^{-2/3}$	$e^{-F\Psi_0/RT}$	$e^{-F\Psi_1/RT}$	$e^{-F\Psi_2/RT}$	$\log K$
$TiOH^{-1/3}$	0	0	0	0	1	0	0	0	0	0
$Ti_2O^{-2/3}$	0	0	0	0	0	1	0	0	0	0
$TiOH_2^{+2/3}$	1	0	0	0	1	0	1	0	0	$\log K_H$
$Ti_2O^{+1/3}$	1	0	0	0	0	1	1	0	0	$\log K_H$
$TiOH^{-1/3}$–Na^+	0	1	0	0	1	0	0	0	1	$\log K_{Na^+}$
$Ti_2O^{-2/3}$–Na^+	0	1	0	0	0	1	0	0	1	$\log K_{Na^+}$
$TiOH_2^{+2/3} - Cl^-$	1	0	1	0	1	0	1	0	−1	$\log K_{Cl^-} + \log K_H$
$Ti_2OH^{+1/3} - Cl^-$	1	0	1	0	0	1	1	0	−1	$\log K_{Cl^-} + \log K_H$
$Ti_2AO7^{+1/3}$	2	0	0	1	2	0	1.5	−0.5	0	$\log K_{AO7}$
$Ti_2(AO7)_2^{-2/3}$	2	0	0	2	2	0	1.5	−1.5	0	$\log K_{AO} + \log K_D$
$Ti_2(AO7)_3^{-5/3}$	2	0	0	3	2	0	1.5	−2.5	0	$\log K_{AO7} + \log(K_D K_{Tr})$
Sum							Σ_0	Σ_1	Σ_2	

of bleaching of $AO7^-$ via a visible light-driven, dye-sensitised process, appears to correlate to some degree with f_{AO7} at different pHs, as expected given that the reaction mechanism implies only dye molecules that are in direct contact with the surface can undergo photodegradation via a dye-sensitised route.

Acknowledgements

The authors thank Professor Bourikas for many useful discussions relating to the MUSIC and CD-MUSIC models of the metal oxide–electrolyte interface.

Appendix A.

Table A1 (below) defines the formation of each species in terms of the following components (columns): dissolved species, surface species and electrostatic components. The latter are defined in terms of the expression $\exp(-F\psi_i/RT)$, with $i = 0$, 1 and 2 for the corresponding planes (see Fig. 3). The species concentrations are calculated using the coefficients in Table A1, where, reading across the table, the general expression for the species concentration, S (units: M) is:

$$[S] = \Pi[[C_k]^{n_k} 10^{\log K} \quad \text{(A1)}$$

where C_k is the component's concentration (units: M), including electrostatic components, $\exp(F\psi_k/RT)$, surface components ($TiOH^{-1/3}$ and $Ti_2O^{-2/3}$) and solution components. The coefficients n_k are in the rows. The final column comprises the relevant expressions for the logarithms of the intrinsic reaction equilibrium constants with, where appropriate, concentration terms of known components.

Briefly the equations in the CD-MUSIC model can be solved using the parameters in Table 1 and the functions generated using Table A1. Thus, it can be shown for titania that:

$$\sum\nolimits_0 = (\rho A/F)(\sigma_o + N_S) \quad \text{(A2)}$$

For a given pH, a set of potentials, ψ_o, ψ_1 and ψ_d (=ψ_2) are chosen so that a value for Σ_1 and then σ_o (via Eq. (A2)) can be calculated.

Similarly, the summations:

$$\sum\nolimits_1 = (\rho A/F)\sigma_1 \quad \text{(A3)}$$

And

$$\sum\nolimits_2 = (\rho A/F)\sigma_2 \quad \text{(A4)}$$

Allow values for σ_1 and σ_2 to be calculated. However, these values must also be related to each other via the following electrostatic equations:

$$\sigma_o = C_1(\psi_0 - \psi_1) \quad \text{(A5)}$$

$$\sigma_1 + \sigma_o = C_2(\psi_1 - \psi_2) \quad \text{(A6)}$$

$$\sigma_0 + \sigma_1 + \sigma_2 + \sigma_{ddl} = 0 \quad \text{(A7)}$$

where

$$\sigma_{ddl}\,(\text{units}\,\mu\text{C cm}^{-2}) = -11.72c^{1/2}\,\sinh(zF\psi_d/RT) \quad \text{(A8)}$$

where c is the background electrolyte concentration. Thus, for any pH, by varying the values of ψ_o, ψ_1 and ψ_d (=ψ_2) eventually a unique set of values for these potentials can be obtained which generate σ_0, σ_1, σ_2 and σ_{ddl} values (via Eqs.: (A2)–(A4) and (A8), respectively) that are the same as those generated using Eqs. (A5) and (A6) and which also satisfy the need for overall electroneutrality, i.e. Eq. (A8). In this work the optimisation process was carried out using an in-house written, macro incorporated in Excel. Others [6,21] use the significantly faster and equally effective ECOSAT program for calculating chemical equilibria. Both approaches generate the same data sets for both basic Stern (i.e. MUSIC) and three plane (CD-MUSIC) model calculations.

In applying the CD-MUSIC model as proposed by Bourikas et al. [6], where $AO7^-$ is assumed to be monomeric in solution and adsorb onto the surface as such, the last 2 surface species rows in Table A1 are not applicable and the value of $K_{AO7\text{-in}}$ used is given in Table 1. In extending this model to allow for the monomers, dimers and trimers of $AO7^-$ present in solution to adsorb equally well onto the surface of the titania, all surface species rows in Table A1 are used, along with the knowledge of the total dye concentration and the fraction of that which, in solution, is in monomeric form (from Fig. 2) and the revised value of $K_{AO7\text{-in}}$ given in Table 1.

References

[1] M.R. Hoffmann, S.T. Martin, W.Y. Choi, D.W. Bahnemann, Chem. Rev. 95 (1995) 69–96, and references therein.
[2] O. Carp, C.L. Muisman, A. Reller, Prog. Solid State Chem. 32 (2004) 33–177.
[3] A. Mills, S. LeHunte, J. Photochem. Photobiol. A: Chem. 108 (1997) 1–35.
[4] C. Bauer, P. Jacques, A. Kalt, Chem. Phys. Lett. 307 (1999) 397–406.
[5] J. Bandara, J.A. Mielczarski, J. Kiwi, Langmuir 15 (1999) 7670–7679.
[6] K. Bourikas, M. Stylidi, D.I. Kondarides, X.E. Verykios, Langmuir 21 (2005) 9222–9230.
[7] K. Rajeshwar, M.E. Osugi, W. Chanmanee, C.R. Chenthamarakshan, M.V.B. Zanoni, P. Kajitvichyanukul, R. Krishnan-Ayer, J. Photochem. Photobiol., B 9 (2008) 171–192.
[8] I.K. Konstantinou, T.A. Albanis, Appl. Catal. B: Environ. 49 (2004) 1–14.
[9] K. Bourikas, private communication, 2009.
[10] M. Stylidi, D.I. Kondarides, X.E. Verykios, Appl. Catal., B 47 (2004) 189–201.
[11] M. Stylidi, D.I. Kondarides, X.E. Verykios, Appl. Catal., B 40 (2003) 271–286.
[12] H. Lachheb, E. Puzenat, A. Houas, M. Ksibi, E. Elaloui, C. Guillard, J.-M. Herrmann, Appl. Catal., B 39 (2002) 75–90.
[13] K. Vinodgopal, D.E. Wynkoop, P.V. Kamat, Environ. Sci. Technol. 30 (1996) 1660–1666.
[14] X. Yan, T. Ohno, K. Nishijima, R. Abe, B. Ohtani, Chem. Phys. Lett. 429 (2006) 606–610.

[15] F. Kiriakidou, D.I. Kodarides, X.E. Verykios, Catal. Today 54 (1999) 119–130.
[16] B. Simončič, J. Špan, Dyes Pigm. 26 (1994) 257–276.
[17] K.M. Kale, E.L. Cussler, D.L. Evans, J. Phys. Chem. 84 (1980) 593–598.
[18] B. Milicevic, G. Eigenmann, Helv. Chim. Acta 14 (1964) 1039–1043.
[19] A.K. Ghosh, P. Mukerjee, J. Am. Chem. Soc. 92 (22) (1970) 6408–6412.
[20] R.L. Reeves, M.S. Maggio, S.A. Harkaway, J. Phys. Chem. 83 (18) (1979) 2359–2368.
[21] K. Bourikas, T. Hiemstra, W.H. Van Riemsdijk, Langmuir 17 (2001) 749–756.
[22] T. Hiemstra, W.H. Van Riemsdijk, J. Colloid Interface Sci. 179 (1996) 488–508.
[23] P. Venema, T. Hiemstra, W.H. Van Riemsdijk, J. Colloid Interface Sci. 181 (1996) 45–59.
[24] G. Li, X.S. Zhao, M.B. Ray, Sep. Purif. Technol. 55 (2007) 91–97.
[25] V. Augugliaro, C. Baiocchi, A.B. Prevot, E. García-López, V. Loddo, S. Malato, G. Marcí, L. Palmisano, M. Pazzi, E. Pramauro, Chemosphere 49 (2002) 1223–1230.
[26] K.R. Gopidas, P.V. Kamat, J. Phys. Chem. 93 (1989) 6428–6433.